Computation of Navier-Stokes Equations for Three-Dimensional Flow Separation

Ching-Mao Hung*
NASA Ames Research Center, Moffett Field, California 94035

Supersonic flows over a sharp and a flat-faced blunt fin mounted on a flat plate are simulated numerically. Several basic issues involved in the resultant three-dimensional steady flow separation are studied. Using the same number of grid points, different grid spacings are employed to investigate the effects of grid resolution on the origin of the line of separation. Various shock strengths are used to study the separation of boundary layer and to establish the existence or absence of secondary separation. The length of separation ahead of the flat-faced blunt fin, bifurcation of a horseshoe vortex, and the accessibility of a closed-type separation are investigated. The usual interpretation of the flowfield from previous studies and new interpretations arising from the present simulation are discussed.

Introduction

IN the past, fluid dynamics has been divided into two branches—theoretical and experimental. Advances in numerical methods and in computer capabilities have now qualified computation as a separate branch of fluid dynamics. Using the computer as a tool, computational fluid dynamics (CFD) is able to supplement the other two branches and to carry out its own research, development, and further advancement in fluid dynamics as a field of physical science. CFD is now on the threshold of definitive explorations—solving the Navier-Stokes equations and finding the details of the flowfield structure and the underlying physical processes.

Three-dimensional flow separation is a challenging CFD problem. Recently, there have been quite a few numerical solutions to the Navier-Stokes equations for complex geometries showing various three-dimensional flow separations. Very often these studies merely present their numerical capabilities and new applications. Instead of dealing with problems involving complicated geometries, the present paper will focus on supersonic flows over sharp or blunt fins mounted on a flat plate. This is one of the most common and important three-dimensional inviscid-viscous interaction problems and recently has attracted a substantial amount of interest (e.g., Refs. 1–7). The primary purpose of this paper is to study in-depth several basic issues regarding three-dimensional flow separation.

To set the stage for discussion, some general concepts of three-dimensional flow separation will be first briefly reviewed. In particular, descriptions of bubble vs free-vortex layer and open vs closed separations will be emphasized. The rest of the paper will then be devoted to discussion of the computed results of three-dimensional separation. The computed results can confirm, demonstrate or illustrate, but cannot rigorously prove a physical concept. For each issue, we will present the usual interpretations from previous studies and discuss our new interpretations arising from the present simulations. We will present not only the results that agree with experimental observations, but more importantly, present results that suggest new conclusions and hopefully lead to a better understanding of fluid dynamics.

Only those three-dimensional viscous flows that are steady in the mean are considered here. The separation to be discussed can be either laminar or turbulent. We presume that the general patterns are similar and the differences are a matter of degree, rather than character. However, in reality, turbulent separation has certain degrees of unsteadiness (e.g., see Ref. 8), which may not be present for laminar flows. Future direct or large-eddy turbulence simulations are needed for further understanding of unsteady turbulent three-dimensional separation.

Classifications of Three-Dimensional Separation

For two-dimensional steady flows, the criterion for the onset of separation is the vanishing of skin friction. For three-dimensional steady flows, the skin friction in general does not vanish, except at limited numbers of critical (or singular) points. This has inspired many researchers to establish a proper definition for flow separation in three dimensions. It is a common observation that a necessary condition for three-dimensional flow separation is the convergence of oil-streak lines onto a particular line. (Nevertheless, it is not a sufficient condition. In a saddle point of attachment, a convergent limiting streamline is a line of attachment.) The questions are 1) how and where this "separation" line starts? and 2) what are the characteristics of this line?

Eichelbrenner[9] suggests that the line of separation is an envelope of limiting streamlines. The region behind the separation is inaccessible to the flow upstream. Maskell[10] also adopted the concept of envelope and classified three-dimensional separation as either a bubble or a free-vortex layer (Fig. 1). For the bubble type, there exists a surface of separation that isolates a quantity of fluid from the main flow. (The surface of separation either reattaches itself onto the solid surface or is closed downstream of the body.) For the free-vortex-layer type, the separation streamlines are the skeleton of a vortex layer and the surface of separation rolls spirally into a discrete region of vorticity.

Note that while the bubble separation is well defined, the free-vortex-layer separation is not. Maskell has never described how and where the free-vortex layer originates by itself. He suggests that combinations of the bubble and free-vortex-layer separation are the most likely flow patterns. Whenever a bubble forms between two distinct lines of separation, a free-

Received April 6, 1990; revision received Nov. 28, 1990; accepted for publication Dec. 18, 1990.

*Research Scientist. Computational Fluid Dynamics Branch. Mail Stop 202A-1. Associate Fellow AIAA.

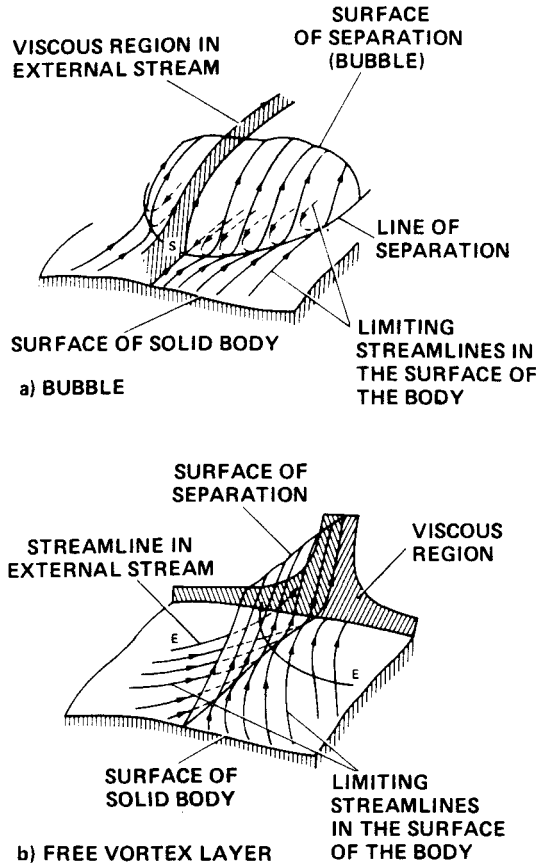

Fig. 1 Classification of three-dimensional separation by Maskell.[10]

vortex layer originates from the bubble surface and a mixed flow results. However, this leads to the controversy of merging two separation surfaces to become a free-vortex layer. It corresponds to the controversy over the intersection of two streamlines at a regular point in two-dimensional flow. Furthermore, while the bubble separation is well-defined, the reattachment of a separation surface itself onto the solid surface, as required for forming a bubble, is structurally unstable. Therefore, the existence of the completely closed separation bubble becomes questionable (see discussion later).

Instead of dealing with the flowfield feature of separation away from the wall, Wang[11] concentrated on the pattern of limiting streamlines near the body surface. He also favored the envelope concept. Based on the accessibility from flow upstream, he classified the separation as closed (inaccessible) or open (accessible). (The concept of bubble and inaccessibility will be critically discussed later.)

Lighthill[12] and Legendre[13] pioneered the theoretical approach and assumed that the pattern of limiting streamlines (or skin-friction lines) as trajectories having properties consistent with those of a continuous vector field. There is one and only one principal trajectory passing through any regular point. Thus, the physics of the vector field are governed by a set of autonomous ordinary differential equations. Also the flow pattern can be characterized by the type and number of singular points and rules governing their relationship. The line of separation is defined as a skin-friction line which issues from a saddle point of separation and, after embracing the body, disappears into a nodal point of separation. Note that "separation" is implicitly defined and described by the flow characteristics at the saddle and nodal points of separation, and along the skin-friction line that connects them. Flow separation in this view has been considered as the convergence of skin-friction lines onto the line of separation. The advantage of this approach is that mathematical theory, such as topological structure, structural stability, bifurcation theory, and qualitative theory of differential equations, can be employed. Lighthill[12] and Legendre[13] still considered a three-dimensional separation inaccessible to the upstream fluid.

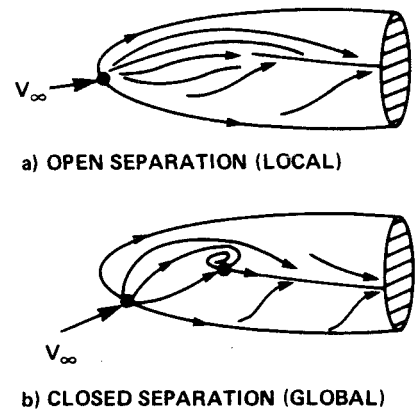

Fig. 2 Open vs closed separation.

Tobak and Peake[14] adopted the concept of convergence of limiting streamline. However, they proposed a distinction between local and global separation. For global separation, as described by Lighthill[12] and Legendre,[13] the line of separation originates from a saddle point of separation and its critical points are in accord with topological theory; for local separation, the line of separation starts from a noncritical point.

As one can see, the so-called global and local separations are very similar, aside from some conceptual differences, to Wang's[11] closed and open separations, respectively. In the present paper, we follow the concept of convergence of limiting streamlines and favor Tobak and Peake's[14] more precise global-and-local definition, but adopt Wang's simple closed-and-open terminology. Therefore, we define (Fig. 2) an open-type separation as that for which the line of separation starts from a noncritical point, while for a closed-type separation the line of separation originates from a saddle point of separation. Note that whether an open separation can start from a regular point is still a matter of current debate. The exact definition and location of the onset of an open separation remain unclear and controversial. The origin of its associated vortex layer and its corresponding vortex core also remain unanswered. It is beyond the scope of this paper to debate these issues.

In most cases, the patterns of the skin-friction lines provide the limiting flow behavior near the body surface, and they enable us to extract certain information about the whole flowfield. However, as pointed out by Dallmann,[15] surface streamline patterns alone cannot provide a unique interpretation of the flowfield. The study of three-dimensional flow separation requires examination of the surface skin-friction lines as well as the external flowfield itself. Numerical computation with graphic techniques provides this requirement and allows one to visualize the entire flowfield in a dynamic sense.

Supersonic Flow Over a Sharp Fin

The first case to be discussed is flow through a shock wave, generated by a sharp fin, glancing across a laminar boundary layer growing over a flat plate (Fig. 3). The governing equations of the analysis are the time-dependent, compressible Navier-Stokes equations incorporating the concept of the thin-layer approximation[16] in all three directions. A numerical procedure developed by Hung and Kordulla[17] is used. The basic numerical scheme is MacCormack's[18] explicit-implicit predictor-corrector algorithm. The solution is carried out until it converges to a steady state. Details of the numerical technique and boundary conditions are discussed in Ref. 17.

Several basic issues concerning the resultant three-dimensional flow separation will be studied. Using the same number of grid points, different grid spacings are employed to investigate the effects of grid resolution on the origin of the line

Table 1 Three grid systems ($57 \times 45 \times 27$, L = 9 cm)

	Coarse	Medium	Fine
Δx min	0.10	0.02	0.01
Δy min	0.0025	0.0025	0.0015
Δz min	0.001	0.001	0.001
Plate leading edge	$I = 4$	$I = 3$	$I = 3$
Fin leading edge	$I = 14$	$I = 22$	$I = 22$

of separation. Various shock strengths (generated by different fin angles) are used to study the so-called separated and unseparated boundary layer and to establish the existence or absence of the secondary separation.

The flow to be simulated has a freestream Mach number $M_\infty = 2.25$, Reynolds number $Re_L = 10^5$, freestream temperature $T_\infty = 263°R$. The flow is assumed laminar and the wall is adiabatic. The apex of the fin (at $x = 0.0$) is placed at a distance $L = 9$ cm from the flat-plate leading edge, which results in a boundary layer about 2.2-mm thick at that location. The distance L is used as the characteristic length in the present study. Here (x, y, z) and (I, J, K) are used in the conventional sense of streamwise, crossflow, and vertical directions. Using the same number of H-grid points ($57 \times 45 \times 27$), three different grid spacings are employed. The coarse grid is uniform in the streamwise direction and geometrically stretched from the fin and plate (in the J and K directions). The medium grid has additional geometric stretching in the streamwise direction from the apex of the fin. The fine grid has finer spacing (compared to the medium grid) near the fin in the J direction and near the apex of the fin in the streamwise direction. To avoid overstretching in the outer region, several zones with different stretching factors are used in the I and J directions. Smooth transition in grid spacing is ensured from one zone to another. The grid spacing parameters are listed in Table 1.

The results of surface pressure are first compared with the experimental and computational results of Degrez,[19] at $y = 5$ cm for a wedge angle $\alpha = 6$ deg (Fig. 4). All results are in good agreement, except that the computed result of Degrez shows a "dip" after the separation. The present results and the experimental data do not show the appearance of the dip in surface pressure. The fine grid result (not shown in Fig. 4) is very close to the medium grid result. This indicates that our grid refinement does not affect the prediction of surface pressure.

Origin of the Line of Separation

Reference 6 contains an extensive study of the flow structure of this geometry for a turbulent boundary layer. It is commonly accepted that the primary separation is a consequence of the high pressure, recovered from the shock system, which induces flow from the fin surface and forces the boundary layer off the flat plate. The question is, where is the origin of the line of primary separation? Figure 5 shows particle traces of Horstman's result, based on a two-equation turbulence model as described in Ref. 6, for the first mesh points above the sidewall ($K = 2$). This particle trace is constructed by a time integration of velocity components restricted to the plane of $K = 2$. Since the plane of $K = 2$ is very close to the flat plate, (normally it would have a resolution smaller than the size of an oil particle), the time integrations are treated as surface particle traces and are considered equivalent to simulation of oil flow in the experiment and simulation of skin-friction lines in the theoretical approach. The particle traces in Fig. 6 indicate that the line of separation originates somewhere in the plate away from the apex of the fin and that this feature is an open-type separation.

Although the global features outside the vicinity of the fin leading edge are similar for the three grid systems, the topologies on the surface near the apex are quite different. Figures 6(a–c) show surface particle traces for the sequence of three grid refinements for the present computation. For the coarse grid, the line of separation also originates from a noncritical point somewhere on the plate and the separation is an open type. As the grid spacing near the leading edge is refined, the starting point of the open-type separation moves. Eventually, as shown in the fine-grid solution (Fig. 6c), the

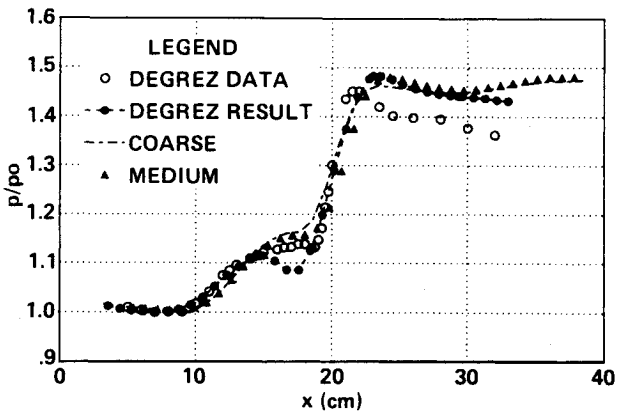

Fig. 4 Comparison of surface pressure at $y = 5$ cm.

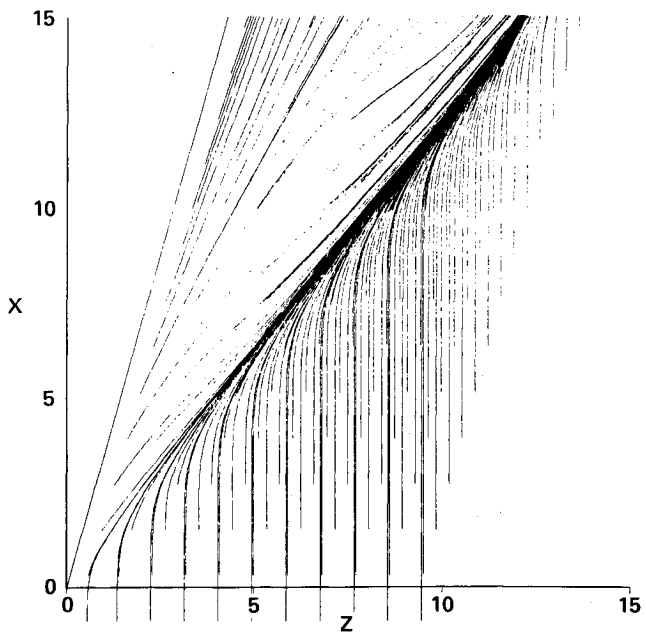

Fig. 5 Surface particle traces by Horstman.[6]

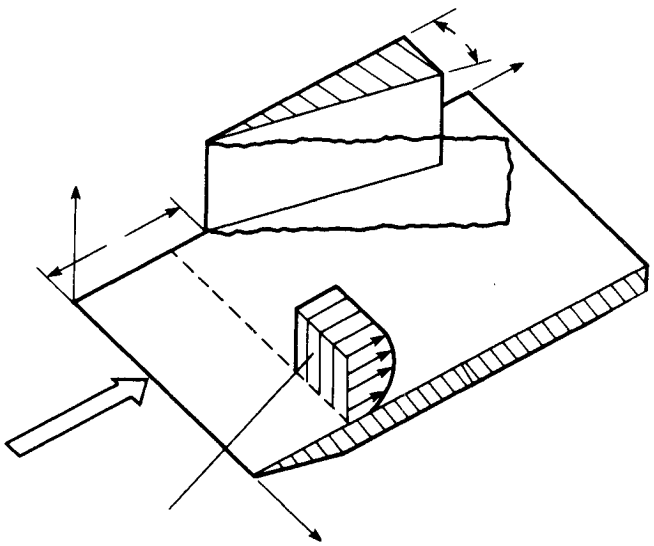

Fig. 3 Supersonic flows over a sharp fin on a plate.

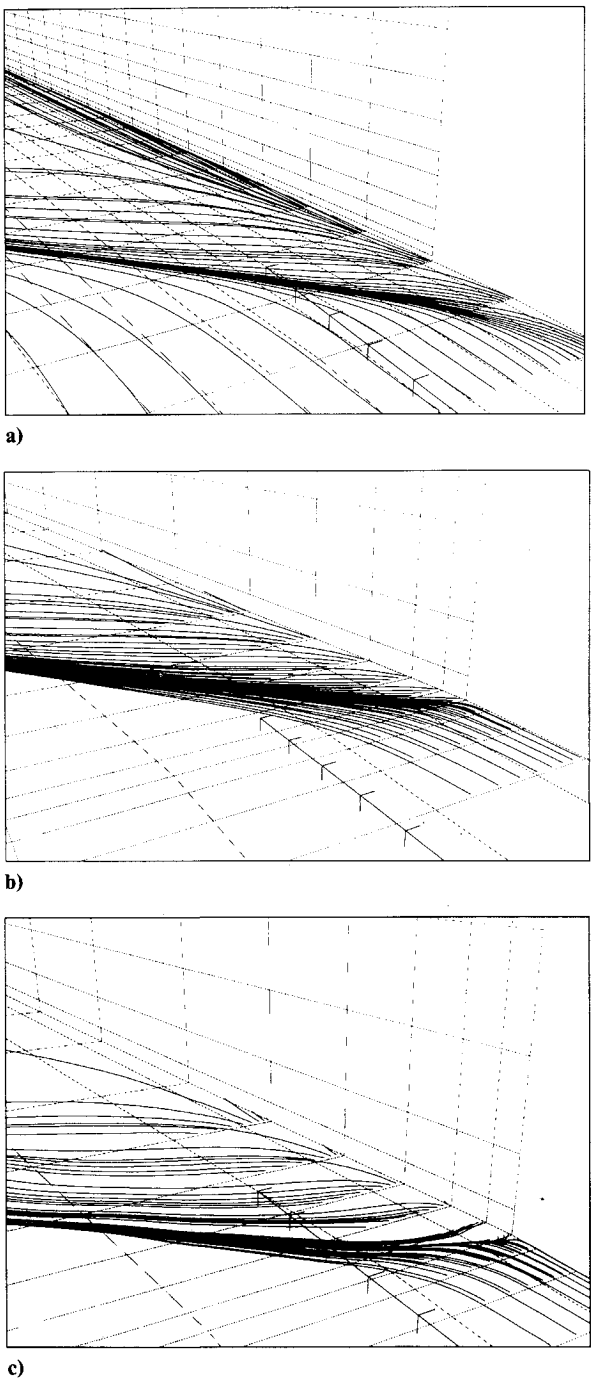

Fig. 6 Surface particle traces (K = 2) for α = 6 deg: a) coarse grid; b) medium grid; and c) fine grid.

line of separation originates from a saddle point and the separation becomes a closed type. This clearly demonstrates that the choice of grid resolution can affect the "calculated" topology. The coarse grid simply cannot resolve the vortex structure, while the fine grid can. As the wedge angle increases to 12 deg, the vortex structure is large enough so that the medium grid (not shown here) is able to reveal a closed-type separation.

Although the existence of an open-type separation is still in question, we believe that some of the numerically observed open-type separations result from insufficient grid resolution. Similarly, experiments also have resolution problems, such as the size of oil droplets. Some of the experimentally observed open-type separations may be the result of low resolution of the device and facility. Hereafter the fine-grid result will be used for discussion, except for cases specially mentioned.

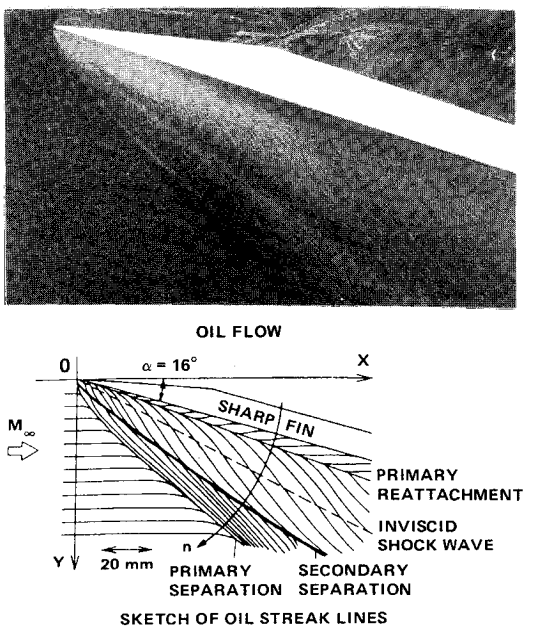

Fig. 7 Surface oil flow by Aso et al.[20]

Secondary Separation

The second question is the existence of a secondary separation. Experiments (e.g., Refs. 20 and 21) very often showed the appearance of another oil-accumulation line behind the line of primary separation, which was interpreted as indicating the existence of a secondary separation (e.g., Fig. 7). The plots of velocity at the first mesh point above the flat plate, K = 2, (Fig. 8a) also show that, in addition to the outermost primary separation line, there is a second "line" of clustering or coalescence of velocity vectors. However, the result of surface particle traces (Fig. 8b) does not display a second line of coalescence, or a secondary separation. Even as the wedge angle increases up to 12 deg (Fig. 9a), the calculations still show no evidence of the existence of secondary separation. Instead, behind the obvious primary separation line, there is a region that the particle traces show strong convergence from one side and weak divergence from the other side. (These traces eventually converge to the primary separation line.) Hence a "band" of high clustering particle traces occurs. From the plot of velocity vectors in the plane K = 2 and plot of surface pressure contours, Figs. 9b and 9c, one can see that the combination of a strong pressure gradient with a pressure plateau leads to a drastic change of the surface skin friction in both magnitude and direction and results in a finite band of converging streamlines.

Note that Degrez's calculation showed a noticeable "dip" of pressure for the 6-deg case (see Fig. 4). When it is strong enough, this drop in pressure can significantly retard the primary separated flow (passing beneath the shock system in the opposite y direction to the main flow) and lead to a secondary separation (see Fig. 12 of Ref. 19). In the present calculation, the pressure shows a plateau region and there is no secondary separation for either the 6- or 12-deg case. (The 12-deg case has a large plateau region with a slight dip of pressure.)

We still do not know whether or not the appearance of secondary oil accumulation in an experiment is caused by a secondary separation. However, an accumulation of oil flow on the surface in an experiment is not necessarily a line of separation, contrary to the usual inference. A drastic change of skin friction in both magnitude and direction could cause a temporal accumulation of oil which would resemble a line of coalescence (e.g., a line of secondary separation). Furthermore, there might be other mechanisms in an experiment, especially for the turbulent case, that could lead to an oil accumulation on the surface. Further detailed studies are needed to answer these questions.

Criterion of Incipient Separation

Whether the boundary layer on the plate is separated or not is usually (e.g., Ref. 22) determined by comparing the turning angle of the limiting streamline with the glancing shock angle in the interaction region. As shown in both Figs. 8b and 9a, there is clearly a line, with clustering of particle traces, that originates from a saddle point with turning angle greater than the angle of the glancing shock, and both flows are considered separated. As the wedge angle decreases, the turning angle of the skin-friction line will decrease and eventually become smaller than the angle of the glancing shock. The flow then will be classified as attached as stated above.

A case with 2-deg wedge angle was calculated with the fine-grid distribution. Figure 10a shows traces of particles whose origins are almost the same as those of the 6-deg case. In contrast to Figs. 6 and 9a, there is no obvious line of convergence of particle traces and the turning of skin-friction lines is smaller than the glancing shock angle; this would conventionally be interpreted as an attached case. However, a close examination of the particle traces near the apex (Fig. 10b) shows that actually the flow is separated. Even though it is very small, the separation is also a closed type, and the structure is topologically the same as that for the previous 6- and 12-deg cases. Actually, all three cases are topologically the same as the structure of a blunt-fin flowfield (see following discussion).

Under certain conditions this type of flow may not separate. However, the conventional method of using the turning angle of the boundary layer equal to the glancing shock angle as the criterion for incipient separation is invalid. Separation does occur before reaching that conventional criterion, as demonstrated above.

Another point should be mentioned here. Figures 12 and 21 of Ref. 7 sketched that, at a low wedge angle, the boundary layer on the sidewall was separated from a saddle point as a closed type of separation on the line of symmetry near the fin apex, and then gradually became attached away from the fin. (This was claimed in Ref. 7 as an open-type separation.) The question arises as to where and how the separation ends. The author believes that, for this case, the definition of sep-

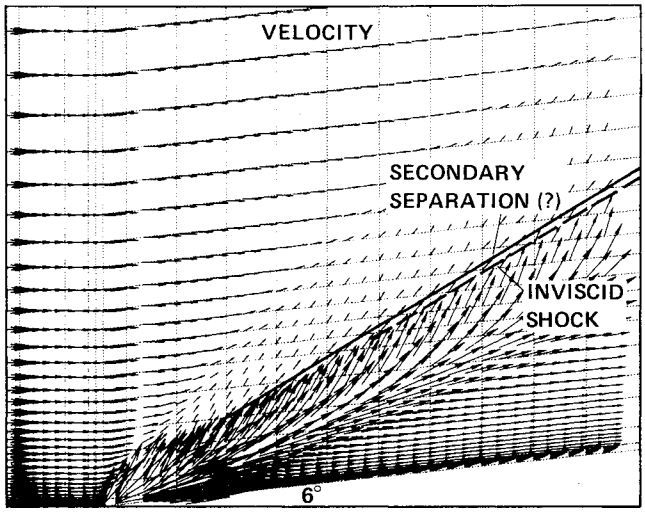

a)

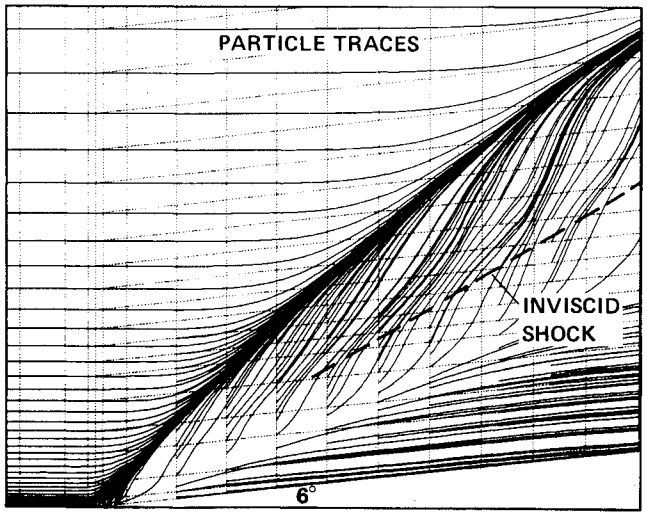

b)

Fig. 8 Velocity vectors and particle traces for $K = 2$ ($\alpha = 6$ deg): a) velocity vectors; and b) particle traces.

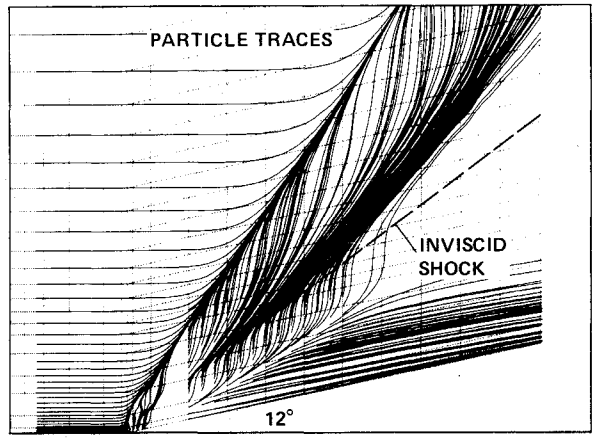

a)

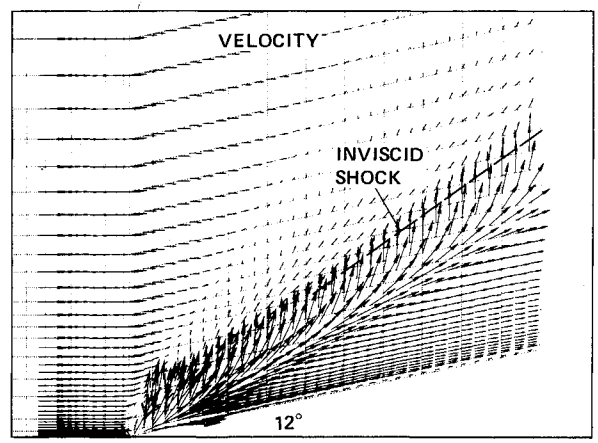

b)

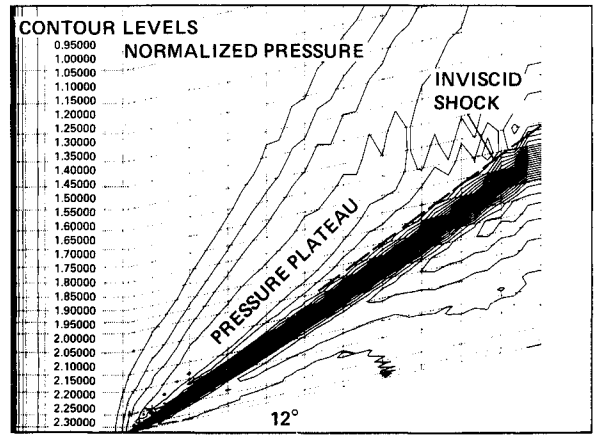

c)

Fig. 9 Flow properties near the wall ($K = 2$) for $\alpha = 12$ deg: a) surface particle traces; b) velocity vectors; and c) pressure contours.

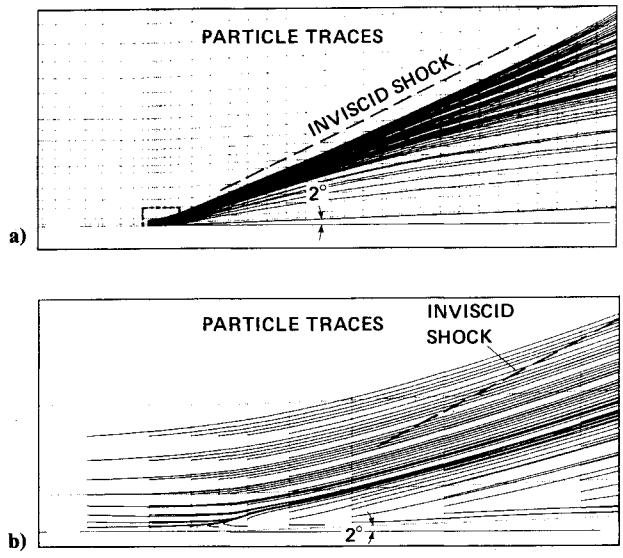

Fig. 10 Surface particle traces (K = 2) for α = 2 deg: a) general features; and b) near apex.

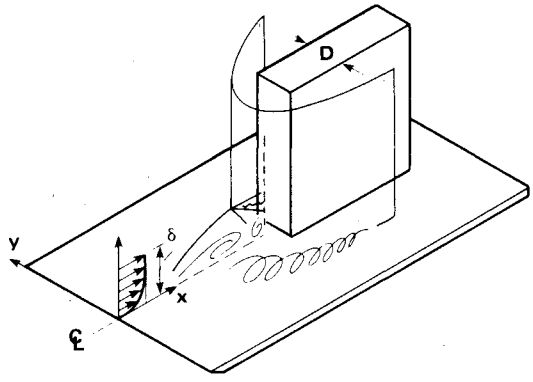

Fig. 11 Supersonic flow over a flat-faced blunt fin on a flat plate.

aration based on turning angle and oil accumulation in the experiment fails. Because of boundary-layer growth on the fin, the shock wave is stronger and hence the pressure rise is higher near the leading edge of the fin than at a position downstream. The difference in pressure rise changes the turning angle and degree of oil accumulation. Based on the concept of continuity, limiting streamlines would not join together except at a singular point. A line of separation, once it originates from a saddle point, will either continue going downstream to infinity or terminate at a singular point. In other words, once it is separated, the flow cannot gradually be reattached without a singular point, according to topological imperatives.

Supersonic Flow Over a Flat-Faced Blunt Fin

The second problem to be presented is supersonic flow over a flat-faced blunt fin mounted on a flat plate (Fig. 11). The bow shock causes the boundary layer to separate from the plate ahead of the blunt fin resulting in a separated flow region composed of horseshoe vortices near the surface and a lambda-type shock pattern ahead of the fin. The shock wave emanating from the separated flow region (separation shock) interferes with the bow shock, and causes intense heating and high pressure locally around the leading edge of the protuberance.

The governing equations are the time-dependent, compressible mass-averaged Navier-Stokes equations. The flows considered are turbulent and an algebraic eddy-viscosity turbulence model by Baldwin and Lomax,[16] with a "modified distance,"[5] is used to close the system of equations. The numerical procedure developed by Hung and Kordulla[17] was

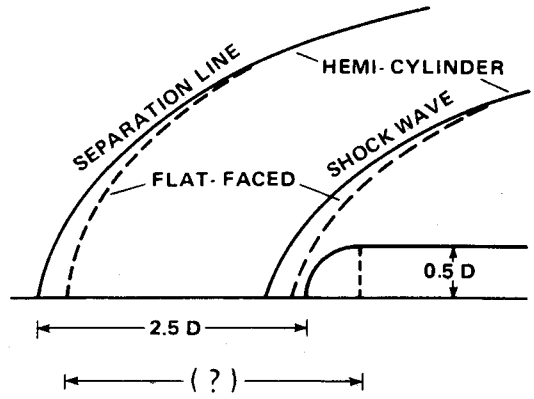

Fig. 12 Sketch of the effects of fin bluntness on separation lines and inviscid shock waves.

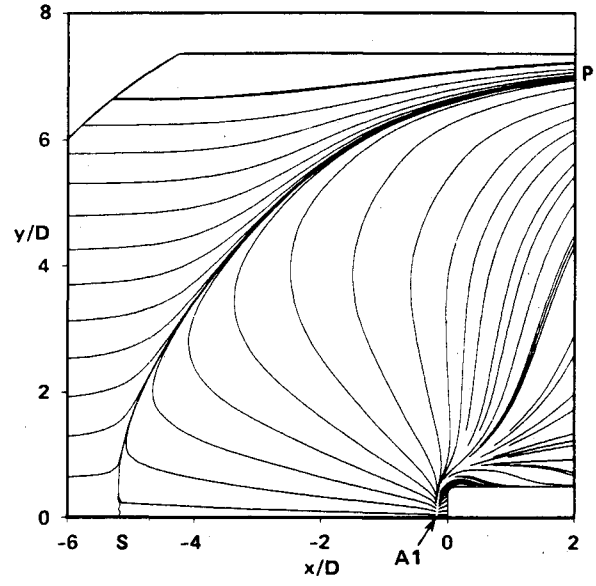

Fig. 13 Surface particle traces (K = 2) for blunt fin.

also used. The flow to be simulated has freestream conditions of M_∞ = 4.9, and unit Reynolds number of 52 × 10^6 m^{-1}. The fin has thickness D = 0.64 cm and is placed 26.7 cm from the leading edge of the flat plate, which results in an incoming boundary-layer thickness of 0.52 cm. A half C-mesh of 40 × 32 × 32 points, similar to that employed in Ref. 5, is used. A variation of mesh spacing, with the same number of points but different stretching, also has been tested. However, the results of surface particle traces and pressure along the line of symmetry (not presented here) are nearly independent of the grid size used. The question of length of separation, structure of horseshoe vortex, and the accessibility of the closed-type separation will be discussed.

Length of Separation

For a hemicylindrical blunt fin, it has been observed from experiments (e.g., Refs. 1 and 4) and numerical simulations (e.g., Ref. 5) that many of the important flow length scales are primarily dependent on the diameter of the fin leading edge D, and only weakly dependent on the freestream Mach number M_∞, and thickness δ, of the incoming boundary layer. Variation of the thickness of the incoming boundary layer by a factor of 10 in Ref. 5 produced approximately the same size of horseshoe vortex and, therefore, the same spatial extent of the interaction. The length of separation along the line of symmetry is about $2.0D$–$2.5D$, provided the incoming boundary layer is turbulent. As the bluntness of the leading edge increases, one can expect the length of separation to increase. The question is how much.

To study the effect of bluntness on the length of separation, let us consider the extreme case, a flat-faced fin. As sketched in Fig. 12, the length of separation is about $2.5D$ on the line of symmetry for a hemicylindrical blunt fin. As the hemicylindrical portion is removed, the bow shock will follow as sketched. Intuitively, one would expect that the location of separation should stay roughly the same. That means the length of separation would increase to about $3.0D$, or slightly less. Surprisingly, it increases even more (by a factor about two for the flat-faced fin). The length of separation is about $5.2D$ for the present computation and about $5.5D$ experimentally.[23] This can be seen clearly in the plots of simulated "oil flow" on the flat plate (Fig. 13). The calculated results confirm the observation from experiments[23-24] of the drastic increase in separation length for flow over a flat-faced fin. Empirically there may be several parameters, such as drag coefficient, and bluntness, to correlate, but basically we still do not understand the reason for this drastic increase.

Existence of Secondary Separation

Figure 14 shows the comparison of surface pressure along the symmetry line for the flat-faced blunt fin. (The plot of the u velocity at the grid points of $K = 2$ is also shown for later discussion.) The agreement between the computed result and the experimental data[23] is reasonably good. The measured

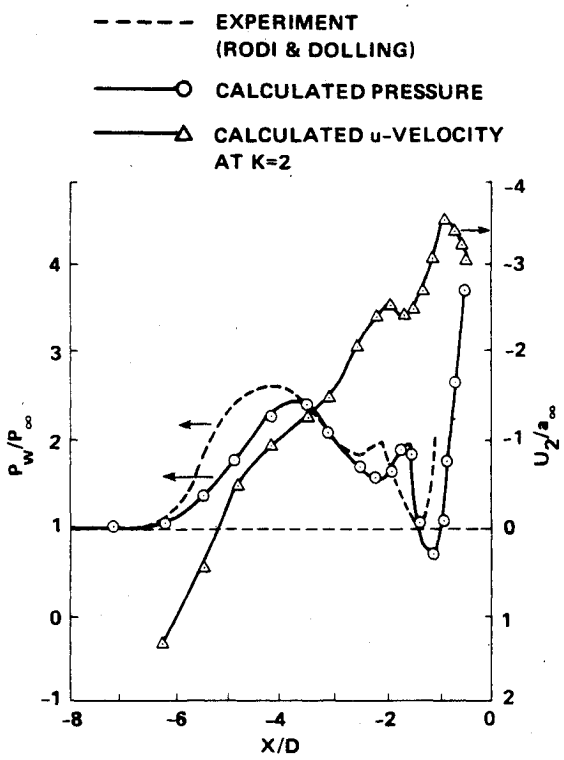

Fig. 14 Comparison of pressure and plot of u velocity at $K = 2$ along line of symmetry.

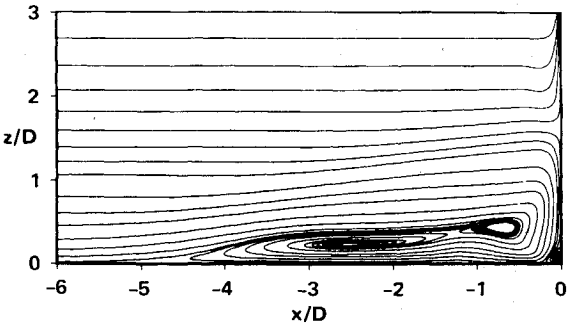

Fig. 15 Particle paths in the plane of symmetry.

pressure shows the appearance of a small second pressure peak (or a "kink"), which, in Ref. 23, was interpreted as an indication of the existence of a secondary separation and the development of an additional pair of vortices. Another question arises with the appearance of a secondary separation. Whenever there is a secondary separation, the issue is whether the main horseshoe vortex will remain as one or bifurcate into two vortices. Sedney and Kitchens[25] suggest that the main horseshoe vortex will bifurcate and that there will be an even number of vortices. The process starts with two vortices—one main horseshoe vortex and one small one near the corner. As secondary separation appears, the main horseshoe vortex bifurcates, and the vortices develop by pairs, in even numbers. For certain flow conditions, the existence of as many as six vortices has been inferred from an experimental oil flow (see Ref. 25).

Figure 15 shows calculated particle paths in the plane of symmetry. The horseshoe vortex does indeed bifurcate into two vortices of the same sign. However, there is no secondary separation under the main horseshoe vortices, and there is an odd number of vortices—three in this case. There are two peaks in the reverse u velocity near the wall ($K = 2$) under the core of these two vortices (see Fig. 14). The reverse velocity near the wall between these two peaks decreases and then increases. That leads to the appearance of a kink in the surface pressure. The present calculation still has, in both the x and y directions, very good grid-point resolution in the region around the pressure kink. Therefore, we do not think that grid-point resolution is an issue in the present computation concerning the nonexistence of a secondary separation.

Under different flow conditions, this decrease of the reverse velocity eventually may lead to a secondary separation. This means that for this type of flow the appearance of a kink in pressure is only a necessary condition for the existence of secondary separation, not a sufficient condition. In other words, even though the pressure field and secondary separation might interact with each other, the secondary separation is generally controlled by the pressure field, rather than vice versa.

Structures of Horseshoe Vortices

It has been generally believed that the structure of horseshoe vortices is in accord with the jet-maze model of Norman,[26] as sketched in Fig. 16a for the case of no secondary separation. The separation point (Fig. 16a) is connected to the outer vortex (indicated as 2). The fluid between a and b, $[a\text{-}b]$, and between c and d, $[c\text{-}d]$ (indicated as 2), is entrained in the outer vortex; the fluid between $[b\text{-}c]$ (indicated as 1) in the inner vortex; and between $[d\text{-}e]$ (indicated as 3) in the third vortex near the corner. The fluid above $[e]$ remains outside the vortices. The structures based on the present calculations (Fig. 15) are resketched for clarity in Fig. 16b. The separation point S ties with the inner vortex (indicated as 1) and the four "layers" of fluid entrained in the three vortices are now marked 1 - 2 - 1 - 3, instead of 2 - 1 - 2 - 3 as in Fig. 16a. (These features of entrainment are discussed in the next section, for the accessibility of a closed-type separation.)

Note that, in Fig. 16b, topologically the attachment point corresponding to the primary separation point S is point A on the fin, and not, as conventionally referred, point $A1$ on the plate. The attachment point $A1$ corresponds to the small separation $S1$ near the corner. If the flow is assumed incompressible, there are lines of zero vorticity joining the separation and attachment points $S - A$ and $S1 - A1$, respectively. It can also be argued that, for an incompressible flow, there are corresponding pressure minima ahead of the separations S and $S1$, and pressure maxima behind the reattachments A and $A1$.

Accessibility and Openness

Based on the earlier observations for computed results, we can delineate the differences between two- and three-dimensional *steady* separation. In two dimensions, the separation

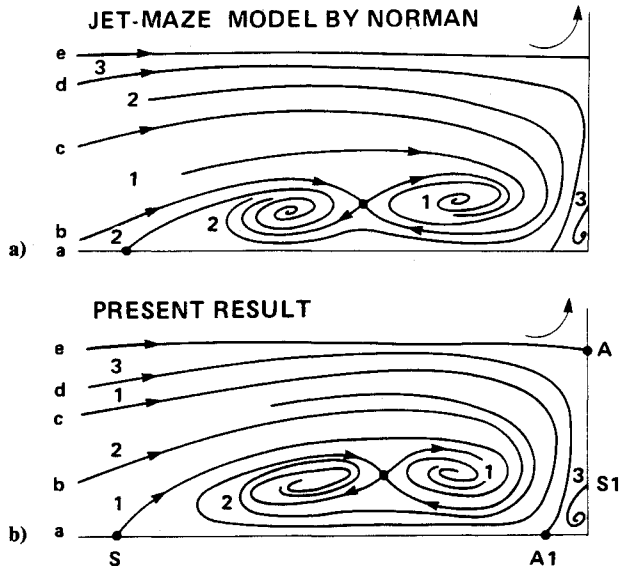

Fig. 16 Structure of horseshoe vortices.

line either connects to a reattachment point and forms a recirculation bubble, or extends to infinity and forms as a wake. In either case, there is a dividing streamline such that the region behind the separation is not a part of the main flow and is *inaccessible* to the upstream fluid particle. In three dimensions this is not true.

In Fig. 13, the critical point S is a saddle point and there is a skin-friction line $S - P$, on the plate, which emanates from point S. This type of separation is classified as a closed-type separation, as described in the classification of three-dimensional separation. Under the influence of the conception of two-dimensional separation, it has been commonly stated that the separation region behind the separation line $S - P$ is inaccessible to the flow coming from upstream (e.g., Refs. 11 and 13). However, this inaccessibility is only valid in the limit of fluid particles moving near/on body surface only. As has been demonstrated earlier, the separation region of this type is accessible to fluid upstream. The skin-friction lines ahead of $S - P$ (Fig. 13) asymptotically approach but cannot get into the region behind the separation line $S - P$. However, based on the concept of limiting streamline, a spiral vortex sheet is generated by an infinite number of streamlines (including the separation line $S - P$ on the surface) emanating from the saddle point S. Because of the spiral nature of the vortex separation, the fluid above the body surface can access the separation region behind $S - P$. In the present case, there are four layers of fluid entraining into three vortices in a manner as shown in Fig. 16b.

Note that the fluid particles separated from saddle point S do not "reattach" to the surface. It is the fluid particles along the "stream tubes" (d) and (e), in Fig. 16b, that attach to the nodal points $A1$ and A on the body and "wet" the plate surface behind the line of separation $S - P$ and the fin surface. Since the fluid particles reaching the attachment points $A1$ and A are not the fluid particles that have previously separated, therefore, in three-dimensional flow, it is an "attachment" point, not a "reattachment" point as used in two-dimensional flow. Note that the term "reattachment" is still widely misused, as in Fig. 7.

Mathematically, the separation point S cannot be connected to its corresponding attachment point A by a single structurally stable streamline, because a connection $S - A$ will result in a closed region concentric around a topological center. Such a feature is a degeneration of a focus and is structurally unstable; i.e., a small perturbation would disrupt the topological structure. (Similarly, it is also true for $S1$ and $A1$.) This situation occurs for two-dimensional separation and reattachment which is structurally unstable and is a transient state of a three-dimensional separation. Based on this, one can argue that there is no *steady* three-dimensional separation that is totally closed by a separation surface. (A perfectly axisymmetric separation is considered as a two-dimensional separation.) There must be some fluid flowing in and some fluid flowing out. All steady three-dimensional surfaces are a kind of vortex sheet in structure. In other words, all steady three-dimensional separations are of the free-vortex-layer type; there is no bubble-type three-dimensional separation as conceived by Maskell.[10]

Finally, we would like to point out that, while separation is defined, attachment is overlooked and there is no definition of "attachment" (even in this study). Very often, an attachment was just treated (e.g., Ref. 27) as a reverse of separation. However, except for some simple flow structures, an attachment process is not a reverse of a separation process, or vice versa, in a three-dimensional separation. As discussed above (Figs., 13, 15, and 16b), the flow separation originates from the saddle point S and has a separation surface (free-vortex layer), with a line of separation on the body surface, which spirals into a vortex or vortices. There is no "attachment surface" associated with the line of attachment in the attachment process. A reversed "separation process" would imply the existence of a stable, spiral-outward vortex core that so far has never been observed in a steady flow. This indicates that a proper definition of attachment is warranted in a three-dimensional flow separation.

Conclusion and Remarks

Computations of supersonic flow over a sharp and blunt fin mounted on a plate were used to study three-dimensional steady flow separation. For the sharp-fin case, separation of the boundary layer on the flat plate was investigated for various grid refinements and fin wedge angles. The calculated results have demonstrated that grid resolution can affect the "calculated" topology. For the coarse grid, the separation is an open type. As the grid spacing near the leading edge is refined, the starting point of the open-type separation moves upstream and eventually the separation becomes a closed type. In the opinion of the author, some of the numerically observed open-type separations (e.g., Fig. 5) result from insufficient grid resolution. Similarly, experiments have resolution problems, and some of the experimentally observed open-type separations may well be due to low resolution of the flow-visualization techniques.

Based on the computation of surface particle traces, no secondary separation was found in the present study. A secondary oil-accumulation line has been conjectured to be a demarcation between regions of high and low surface skin friction.

In a calculation with a 2-deg sharp-fin angle, there is no obvious line of convergent particle traces and the turning angles of skin-friction lines are smaller than the glancing shock angle. This is conventionally interpreted as an attached flow. However, close examination of the particle traces near the apex has shown that the flow is actually separated, and the structure is the same topologically as that for the blunt-fin flowfield.

For the flat-faced blunt fin case, the following observations and conclusions are made.

1) The length of separation increases to about $5.2D$, compared with about $2.0D$–$2.5D$ for the typical hemicylindrical results, and the present numerical results confirm these experimental observations.

2) Even though there is a "kink" in the pressure distribution for the present case, the main horseshoe vortex bifurcates into two and there is no secondary separation under the main horseshoe vortices. In this case three vortices are present; therefore one can conclude that the number of vortices is not always an even number.

3) For the case investigated, the separation point is connected to the inner (downstream) horseshoe vortex, rather

than the outer (upstream) one. The four layers of fluid marked 1 - 2 - 1 - 3 entrain into three vortices as shown in Fig. 16b.

4) The concept of a closed three-dimensional separated region being inaccessible is valid only in the limit of particles moving near/on the body surface. The flow particles above the surface are able to access the separated region through the attachment node and spiral nature of the separation. Indeed, there is no three-dimensional separation that is totally closed by a separation surface; there must be some fluid flowing in and some fluid flowing out. All three-dimensional separation surfaces are a kind of vortex sheet. In general, for three-dimensional separation, an attachment is not the reverse of a separation, or vice versa.

References

[1]Kaufman, L. G., Korkegi, R. H., and Morton, L. C., "Shock Impingement Caused by Boundary-Layer Separation Ahead of Blunt Fin," ARL 72-0118, Wright-Patterson AFB, OH, Aug. 1972.

[2]Hung, C. M., and MacCormack, R. W., "Numerical Solution of Three-Dimensional Shock-Wave and Turbulent Boundary-Layer Interaction," *AIAA Journal*, Vol. 16, No. 12, 1978, pp. 1090–1096.

[3]Horstman, C. C., and Hung, C. M., "Computation of 3-D Turbulent Separated Flow at Supersonic Speed," *AIAA Paper* 79-002, Jan. 1979.

[4]Dolling, D. S., and Bogdonoff, S. M., "Blunt Fin-Induced Shock Wave/Turbulent Boundary-Layer Interactions," *AIAA Journal*, Vol. 20, No. 12, 1982, pp. 1674–1680.

[5]Hung, C. M., and Buning, P. G., "Simulation of Blunt-Fin-Induced Shock Wave and Turbulent Boundary-Layer Interaction," *Journal of Fluid Mechanics*, Vol. 154, May 1985, pp. 163–185.

[6]Knight, D. D., Horstman, C. C., Shapey, B., and Bogdonoff, S., "The Flowfield Structure of the 3-D Shock Wave-Boundary Layer Interaction Generated by a 20-deg Sharp fin at Mach 3," *AIAA Paper* 86-0343, Jan. 1986.

[7]Fomison, N. R., and Stollery, J. L., "The Effects of Sweep and Bluntness on a Glancing Shock Wave Turbulent Boundary-Layer Interaction," AGARD CP 428, Paper 8, 1987.

[8]Dolling, D. S., "Unsteadiness of Supersonic and Hypersonic Shock-Induced Turbulent Boundary-Layer Separation," AGARD-FDP/VKI Special Course on "Three-Dimensional Supersonic and Hypersonic Flows Including Separation," May 8–12, von Karman Inst. of Fluid Dynamics, Brussels, Belgium, 1989.

[9]Eichelbrenner, E. A., "Three-Dimensional Boundary Layers," *Annual Review of Fluid Mechanics*, Vol. 5, 1973, pp. 339–360.

[10]Maskell, E. C., "Flow Separation in Three Dimensions," Royal Aircraft Establishment Rept. Aero. 2565, Nov. 1955.

[11]Wang, K. C., "Boundary-Layer Separation in Three Dimensions," *Reviews in Viscous Flow, Proceedings of the Lockheed–Georgia Company Viscous Flow Symposium*, Marietta, GA, June 1976, pp. 341–414.

[12]Lighthill, M. J., "Attachment and Separation in Three-Dimensional Flow," *Laminar Boundary Layers*, edited by L. Rosenhead, Oxford Univ. Press, London, 1963, pp. 72–82.

[13]Legendre, R., "Regular or Catastrophic Evolution of Steady Flows Depending on Parameters," Rech. Aerosp., Vol. 1982-4, 1982, pp. 41–49.

[14]Tobak, M., and Peake, D. J., "Topology of Three-Dimensional Separated Flows," *Annual Review of Fluid Mechanics*, Vol. 14, 1982, pp. 61–85.

[15]Dallmann, U., "Topological Structure of Three-Dimensional Flow Separations," DFVL R-IB 221-82 A 07, Gottingen, Germany, April 1983.

[16]Baldwin, B. S., and Lomax, H., "Thin-Layer Approximation and Algebraic Model for Separated Turbulent Flows," *AIAA Paper* 78-257, Jan. 1978.

[17]Hung, C. M., and Kordulla, W., "A Time-Split Finite-Volume Algorithm for Three-Dimensional Flowfield Simulation," *AIAA Journal*, Vol. 22, No. 11, 1984, pp. 1564–1572.

[18]MacCormack, R. W., "A Numerical Method for Solving the Equations of Viscous Flow," *AIAA Journal*, Vol. 20, No. 9, 1982, pp. 1275–1281.

[19]Degrez, G., "Computation of a Three-Dimensional Skewed Shock-Wave Laminar Boundary-Layer Interaction," *AIAA Paper* 85-1565, July 1985.

[20]Aso, S., Hayashi, M., and Tan, A. Z., "The Structure of Aerodynamic Heating in Three-Dimensional Shock-Wave/Turbulent Boundary-Layer Induced by Sharp and Blunt Fins," *AIAA Paper* 89-1854, June 1989.

[21]Brosh, A., Kussoy, M. I., and Hung, C. M., "An Experimental and Numerical Investigation of the Impingement of an Oblique Shock Wave on a Body of Revolution," *AIAA Journal*, Vol. 23, No. 4, June 1985, pp. 840–846.

[22]Green, J. E., "Interactions Between Shock Wave and Turbulent Boundary Layers," *Progress in Aerospace Sciences*, edited by D. Kuchemann, Vol. 11, Pergamon Press, Oxford, England, UK, 1970, pp. 235–340.

[23]Rodi, P. E., and Dolling, D. S., "Experimental Study of the Effects of Leading-Edge Geometry on Fin-Induced Turbulent Separated Flow at Mach 5: Preliminary Results," *AIAA Paper* 86-0344, Jan. 1986.

[24]Saida, N., "Separation Ahead of Blunt Fins in Supersonic Turbulent Boundary Layers," IUTAM Symposium on Turbulent Shear Layer/Shock Wave Interaction, Palaiseau, France, Sept. 1985.

[25]Sedney, R., and Kitchens, C. W., Jr., "The Structure of Three-Dimensional Flows in Obstacle–Boundary–Layer Interaction," Flow Separation, AGARD CP-168, Paper 37, 1975.

[26]Norman, R. S., "On Obstacle-Generated Secondary Flows in Laminar Boundary Layers and Transition to Turbulence," Ph.D. Thesis, Illinois Inst. of Technology, Chicago, IL, 1972.

[27]Zhang, Hanxin, "The Separation Criteria and Flow Behavior for Three-dimensional Steady Separated Flow," *Acta Aerodynamica Sinica* (translation), No. 1, March 1985, pp. 1–12.